iScience, Volume *24*

Supplemental information

Host parameters and mode of infection influence outcome in SARS-CoV-2-infected hamsters

Bryan D. Griffin, Bryce M. Warner, Mable Chan, Emelissa Valcourt, Nikesh Tailor, Logan Banadyga, Anders Leung, Shihua He, Amrit S. Boese, Jonathan Audet, Wenguang Cao, Estella Moffat, Lauren Garnett, Kevin Tierney, Kaylie N. Tran, Alixandra Albietz, Kathy Manguiat, Geoff Soule, Alexander Bello, Robert Vendramelli, Jessica Lin, Yvon Deschambault, Wenjun Zhu, Heidi Wood, Samira Mubareka, David Safronetz, James E. Strong, Carissa Embury-Hyatt, and Darwyn Kobasa

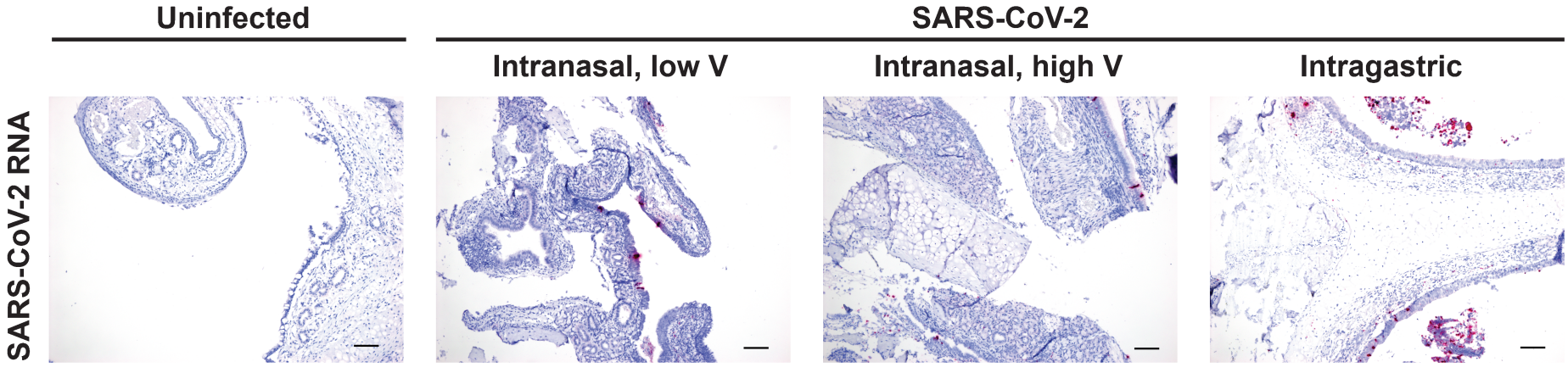

Figure S1. Virus distribution in the nasal turbinates, related to Figure 3. In situ hybridization (ISH) using antisense probes that detect the SARS-CoV-2 genome/mRNA on nasal turbinates tissue of uninfected and SARS-CoV-2-infected hamsters exposed by the indicated routes of infection at 5 dpi. Six-week old mixed female and male golden hamsters were inoculated with 10^5 $TCID_{50}$ of SARS-CoV-2 by a low (20 µl, i.n.L) or high (100 µl, i.n.H) volume intranasal route of administration or an intragastric (i.g.) route of administration and compared to age-matched uninfected controls. Positive detection of viral genomic RNA/mRNA is indicated by magenta staining. The magnification is 10x. Scale bars = 100 µm.

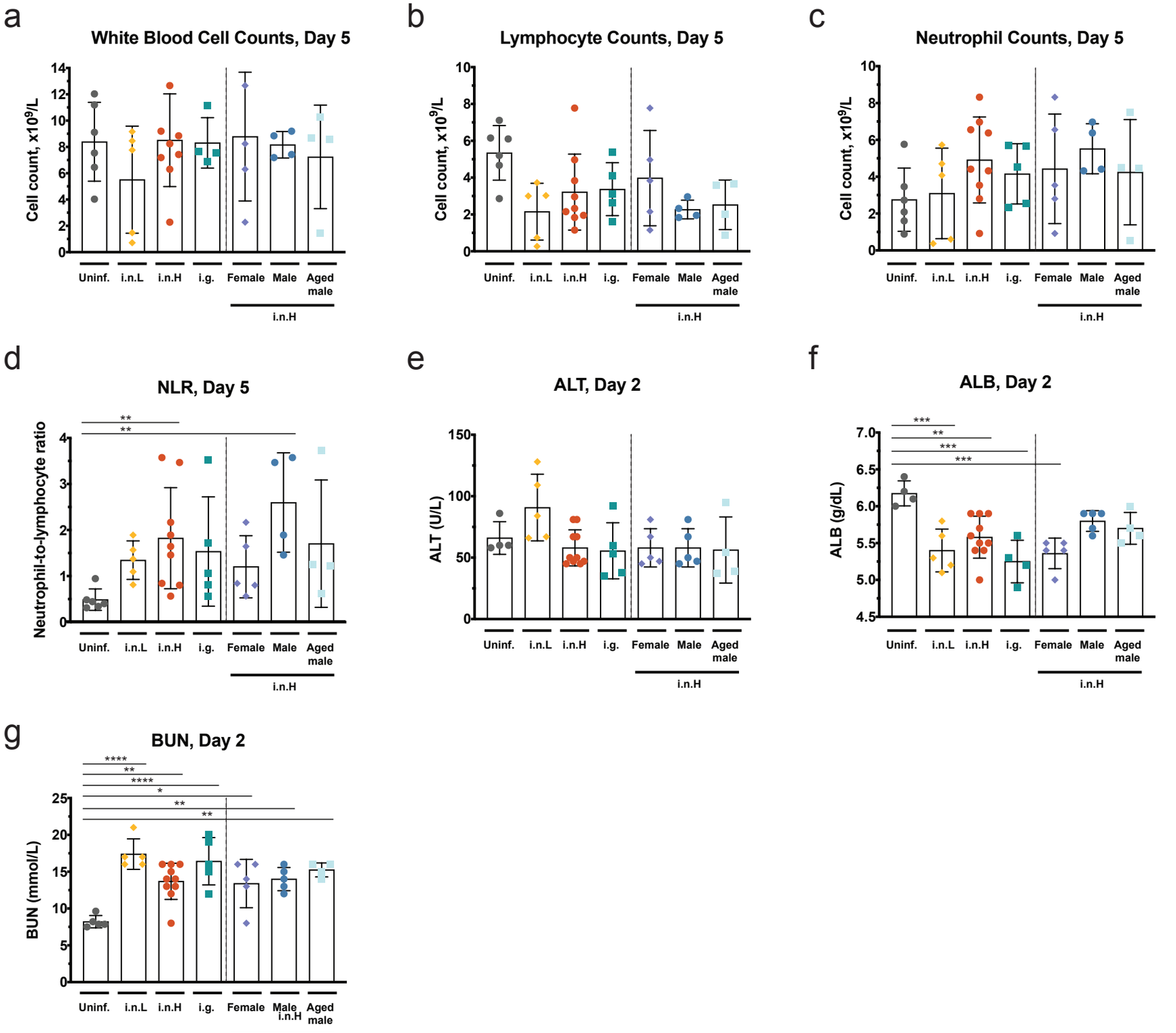

Figure S2. Hematological levels and serum biochemistry in SARS-CoV-2-infected golden Syrian hamsters, related to Figures 1 and 2. Six-week-old male and female hamsters were inoculated with 10^5 $TCID_{50}$ of SARS-CoV-2 by a low volume intranasal (orange diamonds), high volume intranasal (red circles) or intragastric (teal squares) route of administration. The high volume intranasal group data is further broken down by sex (female, lavender;male, dark blue) and compared with an additional group of 20-week-old males exposed to the same dose by a high volume intranasal route of exposure (light blue squares). Hematological levels and serum biochemistry were measured in uninfected and SARS-CoV-2-infected hamsters,including (a) white blood cell counts, (b) lymphocyte counts, (c) neutrophil counts, (d) the neutrophil-to-lymphocyte ratio, (e) alanine aminotransferase (ALT), (f) blood albumin (ALB), and (g) blood urea nitrogen (BUN). Bars indicate mean, error bars indicate SEM. a-d, n = 6, 5,10, 5, 5, 4, and 4 for uninfected, i.n.L, i.n.H, i.g., i.n.H-female, i.n.H-male, and i.n.H-older males, respectively. e-f, n = 4, 5, 10, 5, 5, 5, and 4 for uninfected, i.n.L, i.n.H, i.g., i.n.H-female, i.n.H-male, and i.n.H-older males, respectively. * = P < 0.05, ** P = 0.01, *** P = 0.001, **** = P <0.0001, ns = P > 0.05; unpaired student t test (a-g).

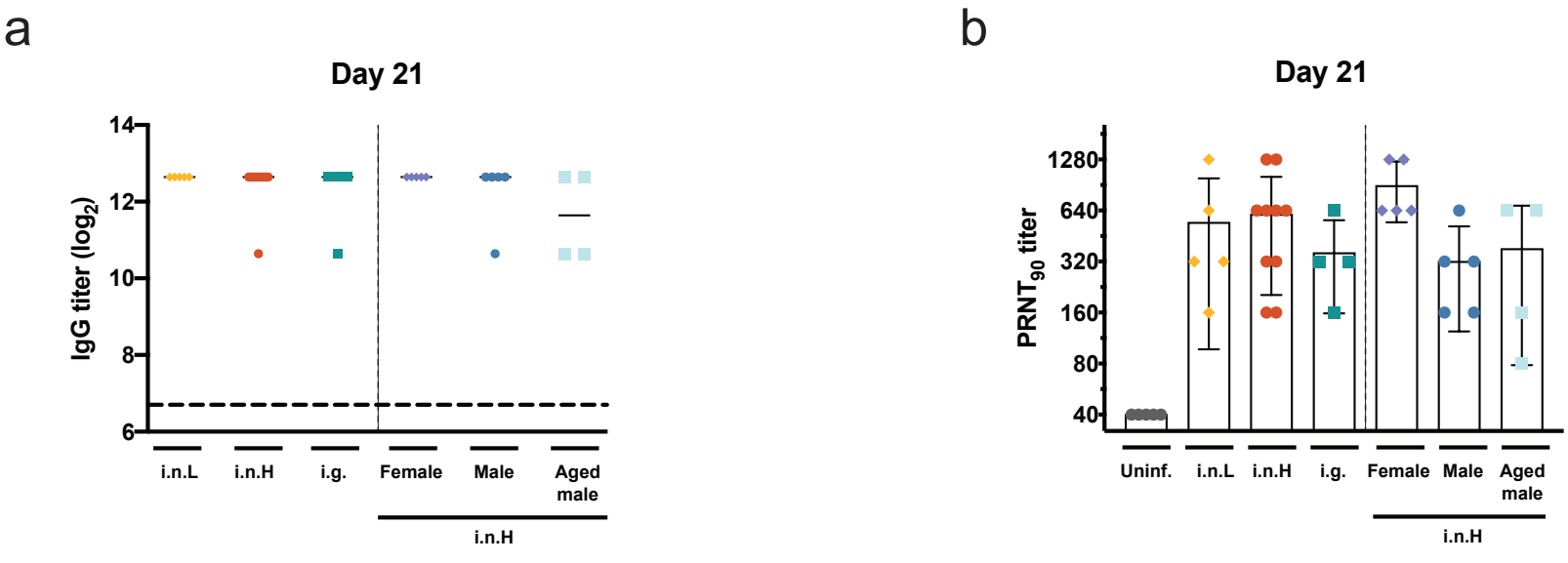

Figure S3. Humoral immune response to SARS-CoV-2 infection at 21 dpi, related to Figures 1 and 2. Six-week-old male and female golden hamsters were inoculated with 10^5 $TCID_{50}$ of SARS-CoV-2 by a low volume intranasal (orange diamonds), high volume intranasal (red circles) or intragastric (teal squares) route of administration. The high volume intranasal group data is further broken down by sex (female, lavender; male, dark blue) and compared with an additional group of 20-week-old males exposed to the same dose by a high volume intranasal route of exposure (light blue squares).**a**, IgG antibody response against SARS-CoV-2 spike antigen were assessed by ELISA using serum collected at 21 dpi. **b**, Neutralizing antibody against SARS-CoV-2 was measured by $PRNT_{90}$ using serum collected at 21 dpi.

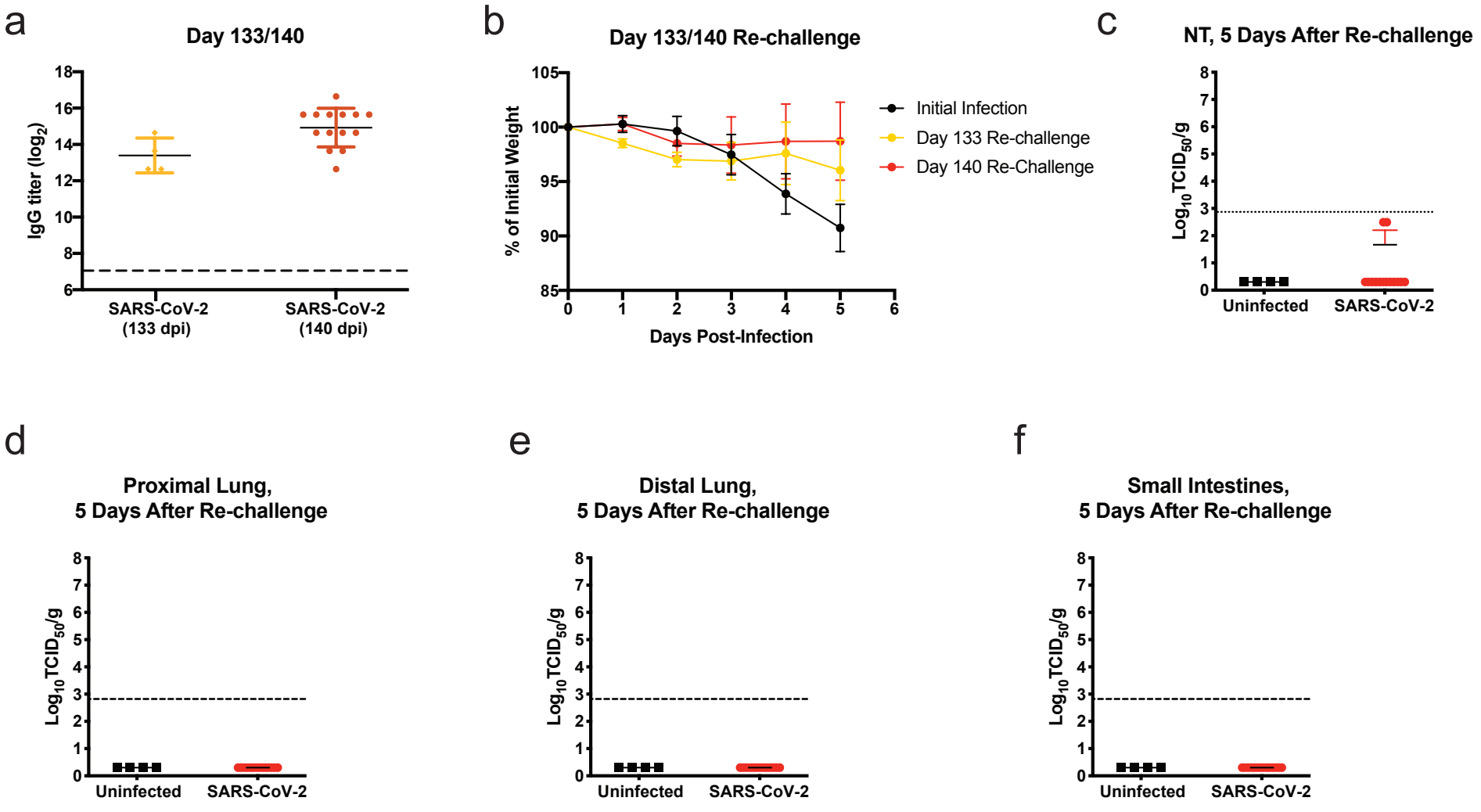

Figure S4. SARS-CoV-2 re-challenge of i.n.H SARS-CoV-2-infected male golden Syrian hamsters at 133/140 dpi, related to Figure 5. Six-week-old male golden hamsters were inoculated with 10^5 $TCID_{50}$ of SARS-CoV-2 by a high volume intranasal (i.n.H) route of administration. Hamsters were monitored for 133 or 140 days at which point they were re-challenged with the same strain of SARS-CoV-2. **a**, IgG antibody response against SARS-CoV-2 spike antigen were assessed by ELISA using serum collected at 133 or 140 dpi, prior to re-challenge. The hamsters were monitored and weighted daily (**b**) until 5 days after re-infection at which point tissues were obtained. The viral burden in the **c**) nasal turbinates, **d**) proximal lungs **e**)distal lung, and **f**) small intestines were determined by infectious $TCID_{50}$ assay.

Table S1. Primers and probes used for detection of viral RNAs and cytokines/chemokines, related to Figures 1, 2, 3, 4, 5, S1.

Oligonucleotides	**Source**	**Identifier**
SARS-CoV-2 E gene primer Forward - 5'-ACAGGTACGTTAATAGTTAATAGCGT-3'	IDT	N/A
SARS-CoV-2 E gene primer Reverse - 5'-ATATTGCAGCAGTACGCACACA-3'	IDT	N/A
SARS-CoV-2 E gene primer Probe - 5'FAM- ACACTAGCCATCCTTACTGCGCTTCG-BBQ-3'	IDT	N/A
IL-1 F - GGCTGATGCTCCCATTCG	IDT	N/A
IL-1 R - CACGAGGCATTTCTGTTGTTCA	IDT	N/A
IL-1 Probe - 6FAM-CAGCTGCACTGCAGGCTCCGAG-BBQ	IDT	N/A
IL-6 F - CCTGAAAGCACTTGAAGAATTCC	IDT	N/A
IL-6 R - GGTATGCTAAGGCACAGCACACT	IDT	N/A
IL-6 Probe - 6FAM-AGAAGTCACCATGAGGTCTACTCGGCAAAA-BBQ	IDT	N/A
TNF-α F - GGAGTGGCTGAGCCATCGT	IDT	N/A
TNF-α R - AGCTGGTTGTCTTTGAGAGACATG	IDT	N/A
TNF-α Probe - 6FAM-CCAATGCCCTCCTGGCCAACG-BBQ	IDT	N/A
IL-2 F - GTGCACCCACTTCAAGCTCTAA	IDT	N/A
IL-2 R - AAGCTCCTGTAAGTCCAGCAGTAAC	IDT	N/A
IL_2 Probe - 6FAM-AGGAAACCCAGCAGCACCTCGAGC-BBQ	IDT	N/A
IFN-γ F - GGCCATCCAGAGGAGCATAG	IDT	N/A
IFN-γ R - TTTCTCCATGCTGCTGTTGAA	IDT	N/A
IFN-γ Probe - 6FAM-CACCATCAAGGCAGACCTGTTTGCTAACTT-BBQ	IDT	N/A
IL-4 F - CCACGGAGAAAGACCTCATCTG	IDT	N/A
IL-4 R - GGGTCACCTCATGTTGGAAATAAA	IDT	N/A
IL-4 Probe - 6FAM-CAGGGCTTCCCAGGTGCTTCGCAAGT-BBQ	IDT	N/A
IL-10 F - GTTGCCAAACCTTATCAGAAATGA	IDT	N/A
IL-10 R - TTCTGGCCCGTGGTTCTCT	IDT	N/A
IL-10 Probe - 6FAM-CAGTTTTACCTGGTAGAAGTGATGCCCCAGG-BBQ	IDT	N/A
FoxP3 R - AAGCAGATCACCTCCTGGAT	IDT	N/A
FoxP3 R - AGCTGCTGCTCCAGAGAC	IDT	N/A
FoxP3 Probe - 6FAM-CACCACTTCTCTCTGGAGGAGGCAC-BBQ	IDT	N/A
STAT2 F - AATGCCTTCAGAGTGTACCG	IDT	N/A
STAT2 R - TGTTCACCGTACTATCCACTTCAT	IDT	N/A
STAT2 Probe - 6FAM-CTGAAGTCAGGACCGCATACTCAGGA-BBQ	IDT	N/A
Mx2 F - CCAGTAATGTGGACATTGCC	IDT	N/A
Mx2 R - CATCAACGACCTTGTCTTCAGTA	IDT	N/A
Mx2 Probe - 6FAM-TGTCCACCAGATCAGGCTTGGTCA-BBQ	IDT	N/A
RPL18 F - GTTTATGAGTCGCACTAACCG	IDT	N/A
RPL18 R - TGTTCTCTCGGCCAGGAA	IDT	N/A
RPL18 Probe - YAK-TCTGTCCCTGTCCCGGATGATC-BBQ	IDT	N/A
RNAscope® Probe- V-nCoV2019-S	Advanced Cell Diagnostics	NC_045512.2
RNAscope® Probe- V-nCoV2019-S-sense	Advanced Cell Diagnostics	NC_045512.2 Cat No. 845701-C2